NASA DEVELOP National Program
Maryland – Goddard

Fall 2022

Bryce Canyon Water Resources

Monitoring Vegetation Health and Water Availability in Bryce Canyon National Park for Drought Stress Mitigation Planning

DEVELOP Technical Report
Final – November 17th, 2022

Aaron Carr (Project Lead)
Alissa Stark
Ashley Grinstead
Melanie Frost

Advisors:
Sean McCartney, Science Systems and Applications, Inc., NASA Goddard Space Flight Center (Science Advisor)

1. Abstract

Bryce Canyon National Park is home to groundwater-dependent ecosystems (GDEs) that are threatened by a multidecadal drought and increased groundwater extraction due to a spike in tourism. These ecosystems contain unique species that are only found in areas where near-surface groundwater is present, such as aspen groves and fens. These species contribute to the high biodiversity found in Bryce Canyon, which boosts an ecosystem's productivity and the services it provides to the park. Unfortunately, many of these GDEs are too small to identify with traditional Earth observation platforms and are difficult to physically reach for monitoring purposes. This project partnered with the National Park Service to identify springs and seeps as a proxy for GDEs within Bryce Canyon from 2013–2022. Furthermore, this project tested the feasibility of various methods to detect and monitor springs and seeps and therefore facilitate the partner's efforts to conserve these ecologically valuable GDEs in Bryce Canyon. The team mapped groundwater discharge with high resolution National Agriculture Imagery Program (NAIP) and assessed park vegetation trends with Landsat 8 Operational Land Imager (OLI) and PlanetScope imagery. *In-situ* precipitation data and the Western Land Data Assimilation System (WLDAS) were used to produce time series of climatic variables. Seeps and spring locations were predicted using random forest classification and maximum entropy machine learning models.

Key Terms

Groundwater dependent ecosystems, remote sensing, NDVI, NDWI, Landsat, WLDAS, high-resolution imagery, Bryce Canyon

2. Introduction

2.1 Background Information

GDEs are defined as communities that rely fully or partially on groundwater and become stressed in the absence of it (Gou et al., 2014; Orellana et al., 2012). GDEs provide structure and function for ecosystems in addition to valuable ecosystem services for humans, such as food production and water purification (Murray et al., 2006). Because of their sensitivity to change, these ecosystems are threatened by drought and anthropogenic activities, such as excessive groundwater pumping (Eamus et al., 2016). Only 19 states have implemented groundwater management legislation, and California is the only state in the United States to formally recognize GDEs in the Sustainable Groundwater Management Act (The Nature Conservancy, n.d.).

Seeps and springs are commonly used as a proxy of where GDEs are located. This project identified springs and seeps from January 2013 to August 2022 in Bryce Canyon National Park, which has an area of 35,835 acres and is located in southern Utah (Figure 1). The park sits at the top of the Paunsagunt Plateau and is split into three distinct ecosystem zones: the spruce/fir forest, the Ponderosa pine forest, and the pinyon-juniper forest. In 2018, visitors contributed $200 million to the local economy and thousands of jobs but also placed a large demand for drinking water and wastewater management (Densmore, 2018). Bryce Canyon also boasts the highest concentration of irregular rock spires ("hoodoos") and is one of the best locations for stargazing in the world. The park was declared an International Dark Sky Park in 2019, spurring a sharp increase in visitors (2,594,904 people in 2019; National Park Service, 2021).

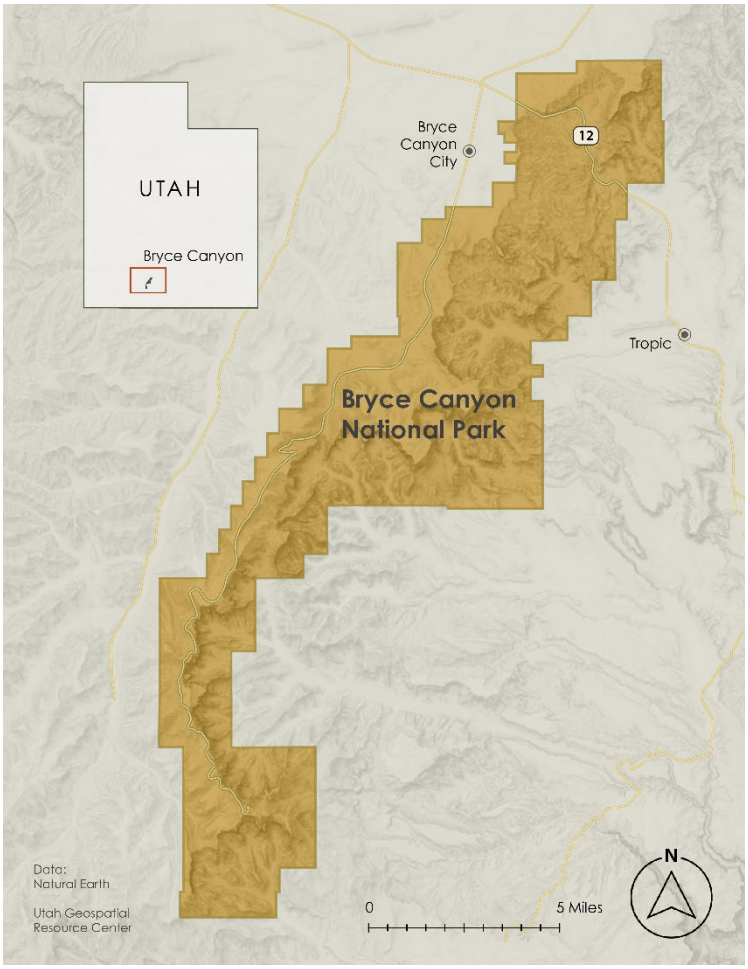

Figure 1. The topography of Bryce Canyon National Park and its location in Utah in the United States of America (from the National Park Service and the Utah Geospatial Resource Center).

To better understand and mitigate the effects of the current multidecadal drought and increased tourism, the National Park Service (NPS) monitors seeps, springs, and GDEs in the park. These ecosystems are often in difficult-to-access areas of the park and only 73 seeps and springs have been identified to date, limiting the breadth of monitoring efforts. Additionally, climatological attributes such as precipitation are only measured in one location of Bryce Canyon, so NPS requested information on changes in surface temperature, soil moisture, evapotranspiration, precipitation, and vegetation health for the last 10 years.

2.2 Project Partners & Objectives

This project partnered with the Bryce Canyon NPS to determine if Earth observations could be used to identify seeps and springs within the park. Remote sensing techniques are not currently utilized by the partners to identify and monitor park hydrology and vegetation. Instead, they manually scour the landscape in Google Earth for indicative "green patches", then verify their presence on foot. ArcGIS Pro is currently used to manage existing, although outdated, hydrologic and vegetation datasets. This project tested the feasibility of various methods to monitor these systems with remote Earth observations, which included the Landsat 8 mission and high-resolution PlanetScope imagery. The team attempted to map springs and seeps as a proxy for GDEs. Change maps were created to analyze trends in the park-wide vegetation. Lastly, the team plotted climate variable time series to investigate pervasive drought conditions. The fulfillment of these objectives will better inform partner management practices by improving their understanding of the location and status of ecologically vital hydrologic and vegetation systems in the park.

3. Methodology

3.1 Data Acquisition

The team acquired Earth observations from the Google Earth Engine (GEE) data catalog and online portals while supplementary datasets were acquired from their respective databases or provided by the partner and collaborators (Table 1). Surface reflectance in the visible and near-infrared (NIR) from the Dove Classic and SuperDove CubeSats in the Planet constellation were filtered and exported within the Planet Explorer API. The team had access to Planet data through NASA's Commercial Smallsat Data Acquisition (CSDA) Program and the images selected approached complete area coverage, minimal cloud cover, and similar off-nadir angles. Planet data was then imported and processed in GEE. Landsat 8 OLI was collected and processed within GEE. NAIP 2021 imagery was collected by county from the Utah Geological Resource Center (UGRC), while 2018 imagery was queried in GEE. WLDAS provided supplementary hydrological data produced through the Land Information System (LIS; Erlingis et al. 2021) which utilizes the Noah-MP land surface model v4.0.1. WLDAS is a model that simulates land surface processes and is intended to inform water stakeholders with near-surface hydrology records in the western United States (Erlingis et al., 2021). Modeled land surface fluxes from 1979 to 2022 were generated within Bryce Canyon bounding coordinates by Dr. Jessica Erlingis and sent through email in netCDF format. A Python script was then used to extract important variables. Park staff also provided *in-situ* weather data from the weather station at the park's visitor center. The partners additionally provided an *in-situ* geospatial dataset of springs and seeps. Light detection and ranging (LiDAR) from Aero-Graphics, Inc. (AGI) was acquired through UGRC, Utah Geological Survey (UGS) provided geologic formations, OpenET provided satellite-based estimates of evapotranspiration for May 2022, and USDA Soil Survey Geographic Database (SSURGO) provided soil type data.

Table 1
Further details on the Earth observations and datasets utilized.

Sensor/Dataset	**Processing Level**	**Dates**	**Acquisition Method**	**Product ID**
PlanetScope Dove Classic PS2 and SuperDove PSB	Level 3B SR	April/May 2017–2022	Google Earth Engine	N/A
Landsat 8 OLI	Level 2 SR Path: 38 Row: 34	2013–2022	Google Earth Engine	LANDSAT/LC08/C02 /T1_L2
WLDAS	N/A	1979–2022	Collaborator	N/A
NPS Bryce Canyon Springs & Seeps	N/A	N/A	Partner	N/A
OpenET	N/A	May 2022	OpenET API	N/A
NAIP	Color Infrared (CIR) bands/Kane and Garfield Counties	2021	UGRC Raster Data Discovery 2.3.2	NAIP2021_Kane_CIR, NAIP2021_Garfield_CIR

NAIP	N/A	2018	Google Earth Engine	USDA/NAIP/DOQQ
LiDAR	N/A	2018	UGRC Raster Data Discovery 2.3.2	N/A
Geological formations	N/A	2022	Provided by partner	N/A
SSURGO	N/A	2016	Web Soil Survey	N/A

3.2 Data Processing

3.2.1 Vegetation Presence and Change

The normalized difference vegetation index (NDVI) is a widely used remote sensing technique for quickly identifying and measuring vegetation health (Huang et al., 2020). Values output by the index range from –1 to +1, with increasingly positive values suggesting healthier vegetation (Dalezios et al., 2000). Increasingly negative values suggest water, and values near 0 are typically bare soil or clouds. Planet imagery was chosen annually from either April or May depending on availability. These months precede the monsoon season, so it was hypothesized that GDEs, which are consistently watered regardless of the time of year, would exhibit a higher NDVI value against contrastingly stressed vegetation. Six sets of annual imagery were downloaded from 2017 to 2022; each of these ranged from three to six images covering the study area and each image included a machine learning-derived Usable Data Masks (UDM2). The images were uploaded into GEE and mosaicked into complete scenes. The 2017 UDM2 was applied to remove cloud from the scene, but the shadow UDM2 did not recognize any clouds within any of the imagery. A random forest model was therefore trained on the 2017 scene with 500 manually selected shadow points and 200 non-shadow points, which produced a validation accuracy of 97% when 80% of the training data was withheld. The model was applicable to each scene due to the consistent annual timing of the imagery. NDVI was then calculated in each image with Equation 1:

$$NDVI = \frac{(NIR - RED)}{(NIR + RED)} \quad (1)$$

where NIR is the reflectance within the NIR spectrum and red is the reflectance within the red spectrum (Rouse et al., 1974). This simple equation harnesses a characteristic of healthy vegetation; it reflects strongly in the NIR and weakly in the red, while stressed and non-vegetation exhibit the opposite. The sampleRegions() function in GEE was used to extract NDVI at each known spring and seep in the 2022 scene for detection analysis. Additionally, a histogram of these data as well as the overall NDVI distribution of the scene were exported from GEE into an Excel comma separated value format. The former dataset was joined to the latter so that bins with at least one spring or seep present were distinguished. NDVI was also calculated from Equation 1 in the Landsat 8 OLI image collection in GEE. The collection was first clipped to the study area and then filtered by year from 2013 to 2022, after which NDVI was applied. The maximum NDVI value was then extracted from each pixel in each year's collection to produce 10 raster layers representative of annual vegetation health. These layers were exported from GEE in GeoTIFF format and imported into ArcGIS Pro. To convert the layers into a single multidimensional raster which was required for the trend analysis they were added to an empty mosaic dataset. The 'Build Multidimensional Raster' tool was then used to establish the year dimension.

3.2.2 Surface Water Presence

Normalized Difference Water Index (NDWI) was used to determine surface water presence in Bryce Canyon (Equation 2). NDWI (Equation 2) has a similar equation to NDVI except it measures the normalized difference between green and NIR (McFeeters, 1996). NDWI values ranged from –1 to 1 where values increasing towards 1 were considered surface water, values decreasing towards –1 meant non-water, and values near 0 were indicative of bare soil.

$$NDWI = \frac{(GREEN - NIR)}{(GREEN + NIR)} \quad (2)$$

When visually looking at a satellite image of Bryce Canyon, there seems to be no noticeable areas of surface water. The team first applied the NDWI (Equation 2) on 0.6-meter NAIP imagery because they wanted to take advantage of the high resolution to see if any type of surface water would give a signal. The team was limited in NAIP imagery availability and, therefore, used the most recent image on GEE, which was August 6, 2018. The NAIP imagery had to first be mosaicked together since it was an image collection and then clipped to the Bryce Canyon boundary shapefile. Additionally, the team applied NDWI on a 3-meter image from Planet in GEE that was taken on August 7, 2018 for comparison of resolutions. Like with NDVI, the team exported histograms of these data as well as the overall NDWI distribution of the scene from GEE into an Excel comma separated value format. The datasets were joined so that bins with at least one spring or seep present were distinguished.

3.2.3 Predictive Modeling

Our partner's framework for identifying seeps and springs from visual inspection (looking for different soil type boundaries and non-coniferous greenness in the dry season) and research in topographical variables' predictive ability of groundwater discharge informed the variables to gather for the project (Downs et al., 2022). The team used ArcGIS Pro to mosaic NAIP CIR imagery from the two Utah counties (Garfield and Kane) which Bryce Canyon Nation Park spans, then created a new NDVI image calculated from the NIR and red bands. LiDAR data spanning the park was downloaded in tiles then mosaicked together. These tiles did not exactly match the entire park, and some sections along the borders – notably the part nearest Bryce Canyon City – were not in this dataset and were excluded from our analysis. This LiDAR image was saved as elevation data and used to calculate the slope of each cell using the ArcGIS geoprocessing tool. Additionally, the team also transformed the soil survey data and the geological features maps to images of distances of each cell to the nearest boundary line between soil type and geological feature. The distribution of each of these datasets is shown in Appendix A1.

3.2.4 Climatic Variable Time Series

The output of the WLDAS model were 1-kilometer resolution netCDF files of monthly surface soil moisture to 10 centimeters, soil moisture 10 centimeters to 40 centimeters, land surface temperature, precipitation rates of snow and rain, snow sublimation, and total evapotranspiration, a summary of which is in Appendix A1. The team aggregated the data by month-year, converted units to be more easily understood (for example, changing Land Surface Temperature to degrees Celsius instead of degrees Kelvin), limited the data to within the park boundaries, and averaged over the park area in Python. These data were then exported into a tabular format for time series charting in Tableau Cloud. An overview of the data collected is in Appendices A3-5.

3.3 Data Analysis

3.3.1 Vegetation and Surface Water Observations

The team reviewed the feasibility of multiple methods to locate seeps and springs. The first two used separate and single attributes—NDVI and NDWI—to attempt to locate groundwater discharge points. A two-tailed difference of means test (Z-Test) was applied to the Planet scenes to determine if the indices at known springs and seeps were statistically unique. The test was also applied to NAIP imagery to confirm that NDWI was not a significant indicator of spring or seep presence because Planet initially suggested that there was no indication of water. The null hypothesis stated that the sample mean (i.e., mean value at pixels containing known springs and seeps across all imagery) equaled the population mean (i.e., mean overall value in all imagery), while the alternate hypothesis stated that they were not equal.

The Mann-Kendall statistical test is used to assess if there is a trend in data over time, in what direction that trend occurs, and if that trend is statistically significant. The calculation of the Mann-Kendall score (S) is an applied method of measuring NDVI change over time (Fassnacht et al., 2019). S is a measure of the difference of value from year to year; negative values indicate a decreasing trend, positive indicate an increasing trend, and 0 indicate no trend. Once annual maximum NDVI was computed from Landsat 8 OLI imagery and placed in a multidimensional format, the team used the 'Generate Trend' function in ArcGIS Pro

to perform trend detection. The tool produced a five-band raster; bands 2 (probability-value [p-value]) and 3 (S) were isolated into their own layers. The team then used the 'Raster Calculator' function to extract all cells of increasing trend, decreasing trend, and of significant trend (p-value ≤ 0.05). Cells of significant increasing and decreasing significant trend were fed into the 'Optimized Hotspot Analysis' function after being converted into a point feature. The use of the Optimized Hotspot Analysis tool within ArcGIS Pro highlighted statistically significant patterns within the Mann-Kendell trends, with hotspots showing clustered increases in trend and cold spots showing clustered trend decreases. The scale of the analysis was calculated within the tool as a fixed distance band determined by the average distance between features, ensuring no more than 30 neighbors within the band, 219 meters for our dataset. Outliers more than three standard deviations are removed by the tool and then the Getis-Ord Gi* (Gi Star) statistic is applied. This produced a feature class that contains p-values, z-scores, and Gi_Bin values. Gi_Bin values are the statistically significant confidence levels for clusters with high and low values determined by the p-values and z-scores. We included the Gi_Bins with the highest confidence levels of 95% and above for both the hotspots and the cold spots (Figure 4).

3.3.2 Predictive Modeling

The team also performed multivariate analyses by running two different model types: random forest classification and maximum entropy. These models incorporated many attributes in presence of known springs and seeps, including NDVI, NDWI, evapotranspiration, soil moisture, ground temperature, precipitation, and topography variables. The random forest approach was selected as it compares the importance of each variable, the model is resistant to multicollinearity, is intuitive when explaining the model, has a built-in validation, and can be run in ArcGIS Pro with distance variables. While the partners provided the team with 73 known seeps and springs or "positive" points, the team created a random dataset of 1,000 points in Bryce Canyon as non-seep/spring or "negative" points. The independent variables considered for the model were NDVI, geological features, distance to geological features changes, elevation, slope, soil types, distance to soil type changes, evapotranspiration, and the precipitation and climatological variables from WLDAS of May 2022. Categorical variables including soil type were discarded as the processing time for running the model exceeded four hours. The parameters selected for the Forest-based Classification and Regression Tool in ArcGIS Pro geoprocessing tools, include compensating for sparse categories, creating 100 trees, and excluding 10% of the data for validation. Once the final model was selected, the team used ArcGIS Pro to create a presence map of predicted seeps and springs throughout Bryce Canyon. A presence-only maximum entropy model was also assessed for feasibility as it has some advantages over the random forest model, including not requiring a "negative" data set, adjusting for the scarcity of seeps/springs to the rest of the park area, and a probability of presence output instead of binary output. The most important independent variables from the random forest model were used in the maximum entropy model. Some of the parameters used in the model include setting a value of 10 presence to 100 background points, choosing a C-log-log function for prediction, and hinge functions applied to the independent variables.

3.3.3 Climatic Variable Time Series

The final portion of the project analyzed trends over time of climatological variables. To analyze the soil moisture, precipitation, surface temperature, and evapotranspiration, the team plotted WLDAS variables using line graphs (Appendix A). Trend lines were added as well for ease of interpretation, and plots were stacked to facilitate comparison across differing y-axis scales.

4. Results & Discussion

4.1 Analysis of Results

4.1.1 Vegetation Presence and Change

NDVI was found to not be a reliable indicator of the presence of springs and seeps on its own. The two-tailed Z-test resulted in a Z-score of +/- 0.271, which is not within the rejection region set by a significance level of 0.05. The p-value of the test (0.787) statistically confirmed this result. The null hypothesis was therefore unable to be rejected, and so NDVI was discontinued as a potential direct detector of springs and

seeps. Figure 2 visualizes the lack of uniqueness of NDVI at known springs and seeps when compared to the overall distribution of the 2022 Planet scene.

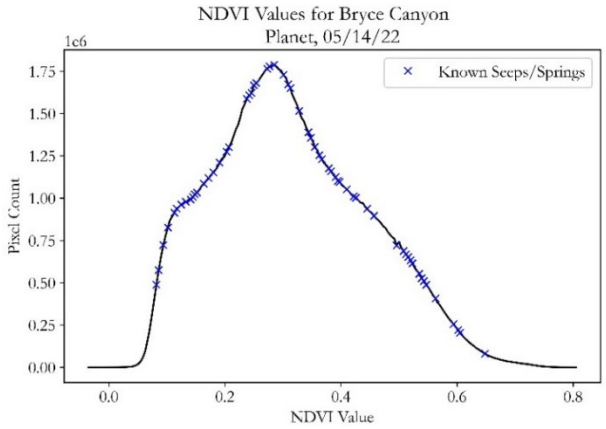

Figure 2. Overall NDVI distribution of a Planet scene from 2022 with known springs and seeps noted.

Bryce Canyon vegetation has increased in health and area between 2013 and 2022 according to the trend analysis. The average annual maximum NDVI value has been on an upward trend since 2013 at a rate of 2.67×10^{-3} with a standard deviation of 0.0225 (Appendix C1). However, this rate of increase is extremely small albeit positive. The Mann-Kendall Trend Test calculated that an area of 16 square kilometers exhibited a significant increase in NDVI. Only 6.8 square kilometers decreased significantly, resulting in a net improvement of 9.2 square kilometers of area within Bryce Canyon (Figure 3). However, most of the park, about 122 square kilometers, had not statistically changed in terms of vegetation health. The Hot Spot Analysis determined where statistically significant clustering of extreme NDVI change in Bryce Canyon has occurred during the study period. One of the more recent large-scale disruptions that occurred in the park, a forest fire that occurred in the south end of the park in 2018, is perceivable in each trend analysis step in Figure 3.

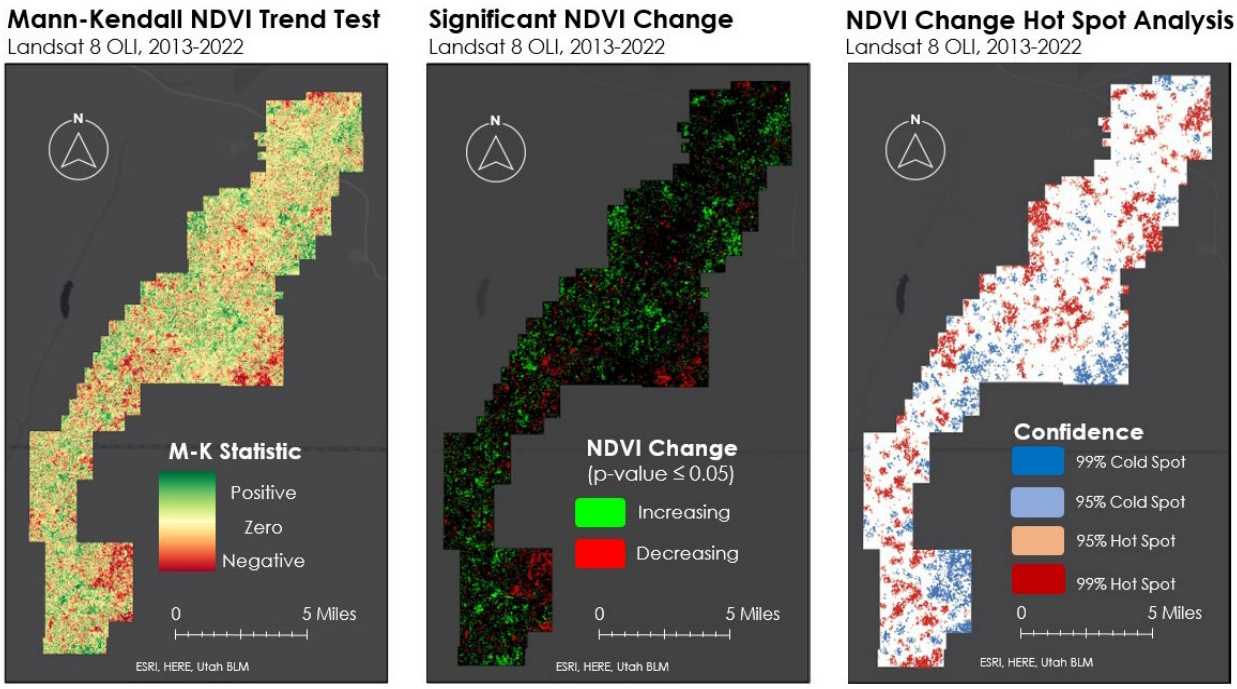

Figure 3. Outputs of the NDVI trend analysis. Mann-Kendall Trend Test (left) indicates increasing, decreasing, and zero trend, while p-values (center) denote those that are statistically significant. The Hot Spot Analysis (right) identified high-confidence clustering of extreme NDVI change.

4.1.2 Surface Water Presence and Change

NDWI was also found to not be a reliable indicator of spring and seep locations, or even detecting the presence of surface water in Bryce Canyon. A two-tailed Z-test for NAIP resulted in a Z-score of +/- 0.151, and the Z-score for Planet was +/- 0.404, which is not within the rejection region set by a significance level of 0.05. This result was confirmed with a P-value of 0.880 for NAIP and 0.686 for Planet. The null hypothesis was therefore unable to be rejected since the P-values were so high, so NDWI was also disregarded as a potential direct detector of springs and seeps. As shown in Figure 4, the distribution of NDWI values for the entire park were below 0 for both the NAIP and Planet imagery. Additionally, NDWI values for the known spring and seep locations were randomly distributed throughout the histogram. Because the NDWI values for the known spring and seep points were not normally distributed, using NDWI to detect the location of springs and seeps proved to be inconclusive.

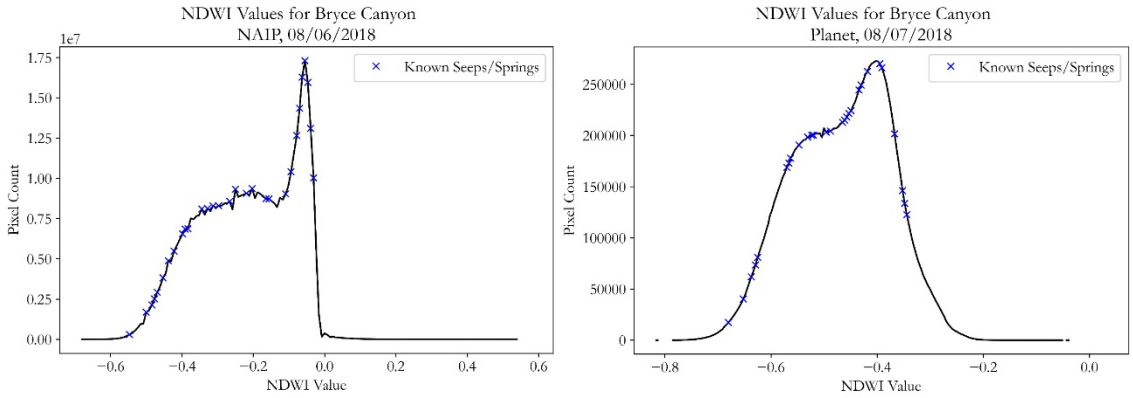

Figure 4. Histogram of NDWI values for the entire park for NAIP and Planet imagery that show the range and the unique NDWI values for known spring and seep locations.

4.1.3 Predictive Modeling

The multivariate models created by machine learning approaches compared explanatory variables potentially useful for identifying seeps and springs. In the random forest classification, the WLDAS precipitation variables were discarded due to lack of variation (as shown in Appendix A3), and the WLDAS climatic data proved to be too coarse for meaningful output mapping. Six explanatory variables: evapotranspiration, NDVI, slope, distance to geological features, elevation, and distance to soil boundaries were kept in the final model, as shown in Appendix B7

The training accuracy of the model was 0.82 while the testing accuracy was 0.81. The resultant map (Figure 5) shows each point (at the coarsest granularity of the explanatory variables, or 30-meters), as blue if the change of a seep or spring is above 50% or gray if the point is less than 50% likely to be a seep or a spring. This map is not particularly useful for the Bryce Canyon National Park partners for ground truthing, as there are too many points over too large of an area without prioritization to be able to survey on foot.

To overcome these challenges, the team used a presence-only maximum entropy model to predict the probability of seeps and springs throughout Bryce Canyon National Park, using the same six explanatory variables from the random forest model. The resultant partial response of the continuous variables is in appendix A5. Seeps and Springs are more likely to occur at lower elevations, closer to geological features and soil boundaries, at slopes between 40 and 80 degrees, and at higher NDVI and evapotranspiration values.

The team chose to use hinge variable expansion on the explanatory variables, as this maximized the area under the response curve (Appendix B5). The cutoff score 0.46 was chosen as it minimized the false positive and false negative predicted values (Appendix B4). The resulting map from the Maximum Entropy model shows the areas of predicted 90-100% probability of seeps and springs throughout Bryce Canyon National Park.

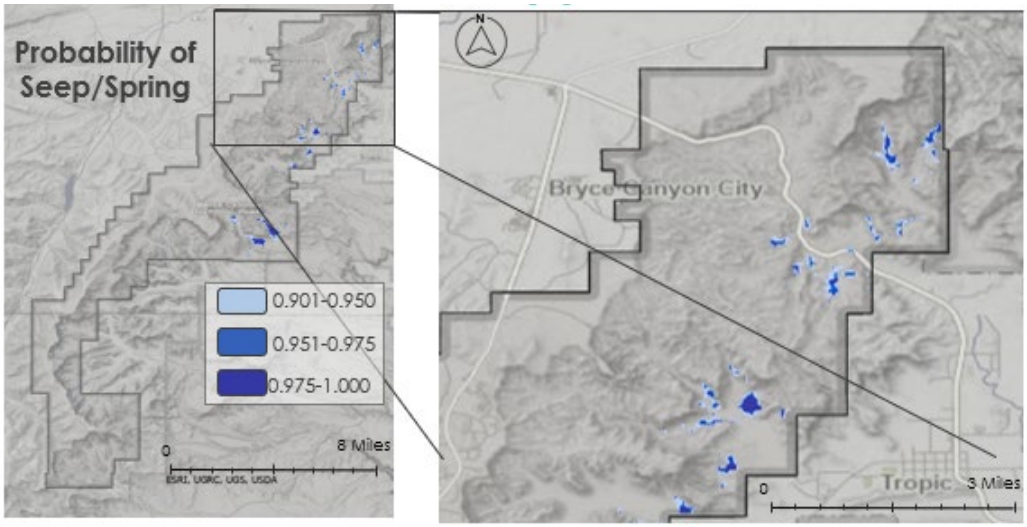

Figure 5. Areas of high probability of seeps and springs as predicted by the Maximum Entropy Model

4.1.4 Climatic Variable Time Series

The final part of the analysis was to investigate climatic variables throughout the park. Rainfall slightly decreased by 9.953 millimeters per year, while snowfall dramatically decreased by 323.7 millimeters per year and snow sublimation did not significantly change at the 0.05 level (Appendix C2). For climatic variables, soil moisture and land surface temperature did not significantly change at the 0.05 level, and evapotranspiration decreased by 34.56 kg per day per year. Trends from the *in-situ* data was less clear, as 2015 and 2019 were

outlying years for precipitation, and the temperature trends were not statistically significant at the 0.05 level (Appendix C3).

4.2 Future Work

There are a handful of alternative approaches that may improve identification of hydrologic and vegetative park features. First, OpenET should be investigated more since a robust analysis was not completed during this project. According to the Random Forest model, evapotranspiration was deemed the most important variable in direct detection of springs and seeps, but the scale of WLDAS is 1-kilometer per pixel. Diving deeper into OpenET's 30-meter evapotranspiration data would hopefully bring forth a more thorough analysis in determining the change in vegetation in the park as well as direct detection of spring and seeps. The team thinks that if groundwater dependent ecosystems are reliant on a different water source than other vegetation in the park, there would be increased evapotranspiration in those areas.

Park stratigraphy may also be a reliable indicator of spring and seep occurrences. The partner has observed that these systems often occur along fault lines and/or above an impermeable layer in the Straight Cliffs formation. However, park stratigraphic maps only describe the relative order of whole formations, and a deeper understanding of subsurface lithology is necessary to predict groundwater discharge (Downs et al., 2022).

Future researchers can utilize remote sensing and updated geological data to determine suitable locations of springs and seeps with a potential for high accuracy. Different machine learning approaches including the deep learning object-detection embedded tools in ArcGIS Pro may allow detection by considering more variables than NDVI or NDWI alone and interaction effects between variables. Using Python or R packages specifically for statistical (probit regression) and machine learning approaches (random forest and clustering), may allow fine tuning of parameters and more insight into predicting the location of seeps and springs.

Future work should also consider a different approach to direct detection of springs and seeps using NDVI as the only indicator. The partner has previously been able to visually detect groundwater discharge by observing relatively greener patches of vegetation in Google Earth. This project only attributed one NDVI pixel to each known spring and seep. An analysis that accounts for surrounding pixels to delineate these islands of greenery may prove more able to automate their workflow. Future projects should utilize a balance of accessible high spatial and temporal resolution Earth observations to have the best opportunity to sense the relatively small features of interest. For example, superimposing known springs and seeps on top of the Hotspot Analysis can assess if vegetation health around groundwater discharge points is on a significant trend of change. However, while Landsat provides a balance of accessibility and temporal resolution, it does not provide an ideal resolution for monitoring individual sites. NAIP is capable of replicating this monitoring method at a much higher resolution, but its temporal availability would hinder the preliminary Trend Analysis required for the Hot Spot analysis.

Finally, the NPS can investigate requesting an airborne sensor to collect aerial thermal imagery since groundwater tends to have an identifiable thermal signature due to having a constant temperature throughout the year (Anderson, 2005). High resolution aerial thermal imagery would be ideal for identifying springs and seeps but would not provide regular periodic imagery for comparison over time.

5. Conclusions

Springs and seeps in Bryce Canyon National Park do not exhibit a statistically unique NDVI or NDWI value, and these two indices alone can therefore not be used to directly detect their presence with the chosen methodology. However, NDVI trend analyses indicate that overall vegetation health had a net increase in area and a slight increase in magnitude since 2013 despite pervasive drought conditions. Machine learning approaches predicted the location of seeps and springs throughout the park based on evapotranspiration, NDVI, elevation, slope, distance to soil boundaries and geological formations. Rainfall has slightly increased by one inch per year since 1979, but snowfall has fallen at a rate of approximately 12 inches per year. *In-situ*

data was inconclusive for overall trends but showed an increase in precipitation in 2015 and 2019, which corresponded with an increased NDVI throughout the park. This project has provided the partners with a description of the spatial change and distribution of springs, seeps, and GDEs within Bryce Canyon. Remote sensing techniques have not previously been tested for their feasibility in identifying and monitoring these ecologically vital systems. Therefore, NPS staff will be able to make more efficient management decisions with both the products from this project and the knowledge of how to reproduce them.

6. Acknowledgments

The Bryce Canyon Water Resources team would like to express their appreciation and thanks to Tyra Olstad, Brett Cockrell, and Eric Vasquez at the National Park Service. Additionally, they would like to acknowledge their science advisor Sean McCartney, and their fellow Carli Merrick for their guidance and enthusiasm throughout this project. The team would also like to thank Dr. Jessica Erlingis from the University of Maryland and Goddard Space Flight Center for their collaboration in integrating WLDAS into the project. Finally, Dr. Nicole Ramberg-Pihl coordinated with the National Park Service and originated this project, and the team is grateful for her work laying the foundation.

This work utilized data made available through the NASA Commercial Smallsat Data Acquisition (CSDA) Program.

This material is based upon work supported by NASA through contract NNL16AA05C.

7. Glossary

Change map – map where differences in a particular variable (ex: soil moisture) are calculated and plotted, highlighting the magnitude and area of change occurrence
Earth observations – Satellites and sensors that collect information about the Earth's physical, chemical, and biological systems over space and time
Ecosystem services – life-sustaining services provided by natural ecosystems to humans
Evapotranspiration – process by which water from the ground is transferred to the air through plant transpiration and evaporation from leaves and soil
GDE – Groundwater dependent ecosystem
GEE – Google Earth Engine
MODIS – Moderate Resolution Imaging Spectroradiometer
NDVI – Normalized Difference Vegetation Index
NDWI – Normalized Difference Water Index
NetCDF – Network Common Data Form file
Random forest classification – machine learning process to classify a variable between groups by iterating over many decision trees
Soil moisture – water in the upper 10 centimeters of soil
Springs/seeps – water reaching the surface from underground
Watershed – area of land that channels precipitation and snowmelt into outflow points via rivers, creeks, and streams
WLDAS – NASA Land Information System model incorporating land surface, meteorology, and satellite data to make daily estimates of water distribution

8. References

Anderson, M. P. (2005). Heat as a Ground Water Tracer. Groundwater, 43(6), 951–968. https://doi.org/10.1111/j.1745-6584.2005.00052.x

Dalezios, N.R., Domenikiotis, C., Kalaitzidis, C., Loukas, A., Tzortzios, S.T. (2000). Cotton Yield Estimation Based on NOAA/AVHRR Produced NDVI. Phys. Chem. Earth, 26(3), 247-251. https://doi.org/10.1016/S1464-1909(00)00247-1

Densmore, P. (2018, May 14). *Bryce Canyon tourism creates over $256 million in economic benefits*. National Parks Service. https://www.nps.gov/brca/learn/news/bryce-canyon-tourism-creates-over-256-million-in-economic-benefits.htm#:~:text=A%20new%20National%20Park%20Service%20%28NPS %29%20report%20shows,economic%20benefit%20has%20doubled%20in%20value%20since%202012

Downs, J., Gerlach, M.E., Guerrón-Orejuela, E.J., Kleindl, W.J., Landry, S.M, & Rains, K.C. (2022). Using Remote Sensing and Machine Learning to Locate Groundwater Discharge to Salmon-Bearing Streams. *Remote Sensing.* 14(1):63. https://doi.org/10.3390/rs14010063

Eamus, D., Fu, B., Springer A., E, & Stevens, L.E. (2016). Groundwater dependent ecosystems: Classification, identification techniques and threats. In A.J. Jakeman, O. Barretaeu, R. J. Hunt, J.D. Rinaudo, A.R. Ross (Eds.), *Integrated Groundwater Management: Concepts, approaches, and challenges* (pp. 313-346)SpringerOpen. 10.1007/978-3-319-23576-9

Erlingis, J.M., Rodell, M., Peters-Lidard, C.D., Li, B., Kumar, S.V., Famiglietti, J.S., Granger, S.L., Hurley, J.V., Liu, P.-W., and Mocko, D.M. (2021, October). A High-Resolution Land Data Assimilation System Optimized for the Western United States. *Journal of the American Water Resources Association* 57 (5): 692–710. https://doi.org/10.1111/1752-1688.12910

Fassnacht, F. E., Kattenborn, T., Schiller, C., Qu, J., Zhao, X. A Landsat-based Vegetation Trend Product of the Tibetan Plateau for the Time-Period 1990-2018. Sci Data, 6(78.) https://doi.org/10.1038/s41597-019-0075-9

Gou, S., Gonzales, S., & Miller, G. R. (2014). Mapping Potential Groundwater-Dependent Ecosystems for Sustainable Management. Groundwater, 53(1), 99–110. https://doi.org/10.1111/gwat.12169

Huang, S., Hupy, J. P., Shao, G., Tang, L., Wang, Y. (2020). A commentary review on the use of normalized difference vegetation index (NDVI) in the era of popular remote sensing. Journal of Forestry Research, 32, 1-6. https://doi.org/10.1007/s11676-020-01155-1

Kelson, R. (2018, May 17). *2018 Utah LiDAR Acquisition - Completed*. Utah Geospatial Resource Center. https://gis.utah.gov/2018-utah-lidar-acquisition

McFeeters, S. K. (1996). The use of the Normalized Difference Water Index (NDWI) in the delineation of open water features. International Journal of Remote Sensing, 17(7), 1425–1432. https://doi.org/10.1080/01431169608948714

Murray, B. R., Hose, G. C., Eamus, D., & Licari, D. (2006). Valuation of groundwater-dependent ecosystems: A functional methodology incorporating ecosystem services. Australian Journal of Botany, 54(2), 221–229. https://doi.org/10.1071/BT05018

NASA Shuttle Radar Topography Mission (SRTM)(2013). Shuttle Radar Topography Mission (SRTM) Global. Distributed by OpenTopography. https://doi.org/10.5069/G9445JDF. Accessed: 2022-11-17

National Parks Service. (2021). Stats report viewer: Annual park recreation visits (1929 – Last calendar year): Bryce Canyon National Park [Dataset]. https://irma.nps.gov/STATS/Reports/Park/BRCA

Orellana, F., Verma, P., Loheide II, S. P., & Daly, E. (2012). Monitoring and modeling water-vegetation interactions in groundwater-dependent ecosystems. Reviews of Geophysics, 50(3). https://doi.org/10.1029/2011RG000383

Planet Team (2017). Dove Classic Level 3A Surface Reflectance [Dataset]. Planet Explorer. Retrieved October 2022, from https://api.planet.com.

Planet Team (2017). Super Dove Level 3A Surface Reflectance [Dataset]. Planet Explorer. Retrieved October 2022, from https://api.planet.com.

Rouse, J. W., Haas, R. H., Schell, J. A., Deerling, D. W. (1974). Monitoring vegetation systems in the great plains with ERTS. NASA. *Goddard Space Flight Center 3d ERTS-1 Symp., Vol. 1*(A). https://ntrs.nasa.gov/citations/19740022614

Soil Survey Staff, Natural Resources Conservation Service, United States Department of Agriculture. Web Soil Survey. Available online at https://websoilsurvey.sc.egov.usda.gov/. Accessed November 2022.

The Nature Conservancy. Groundwater Dependent Ecosystems. | California Conservation Science. (n.d.). Retrieved October 4, 2022, from https://www.scienceforconservation.org/science-in-action/groundwater-dependent-ecosystems-story

US Geological Survey. (2013). Landsat 8 Operational Land Imager (OLI) Level 2, Collection 2, Tier 1 Surface Reflectance [Dataset]. Earth Engine Data Catalog/USGS. Retrieved October 2022, from doi.org/10.5066/P9OGBGM6

9. Appendices

Appendix A – *Univariate and Bivariate Exploration of WLDAS data*

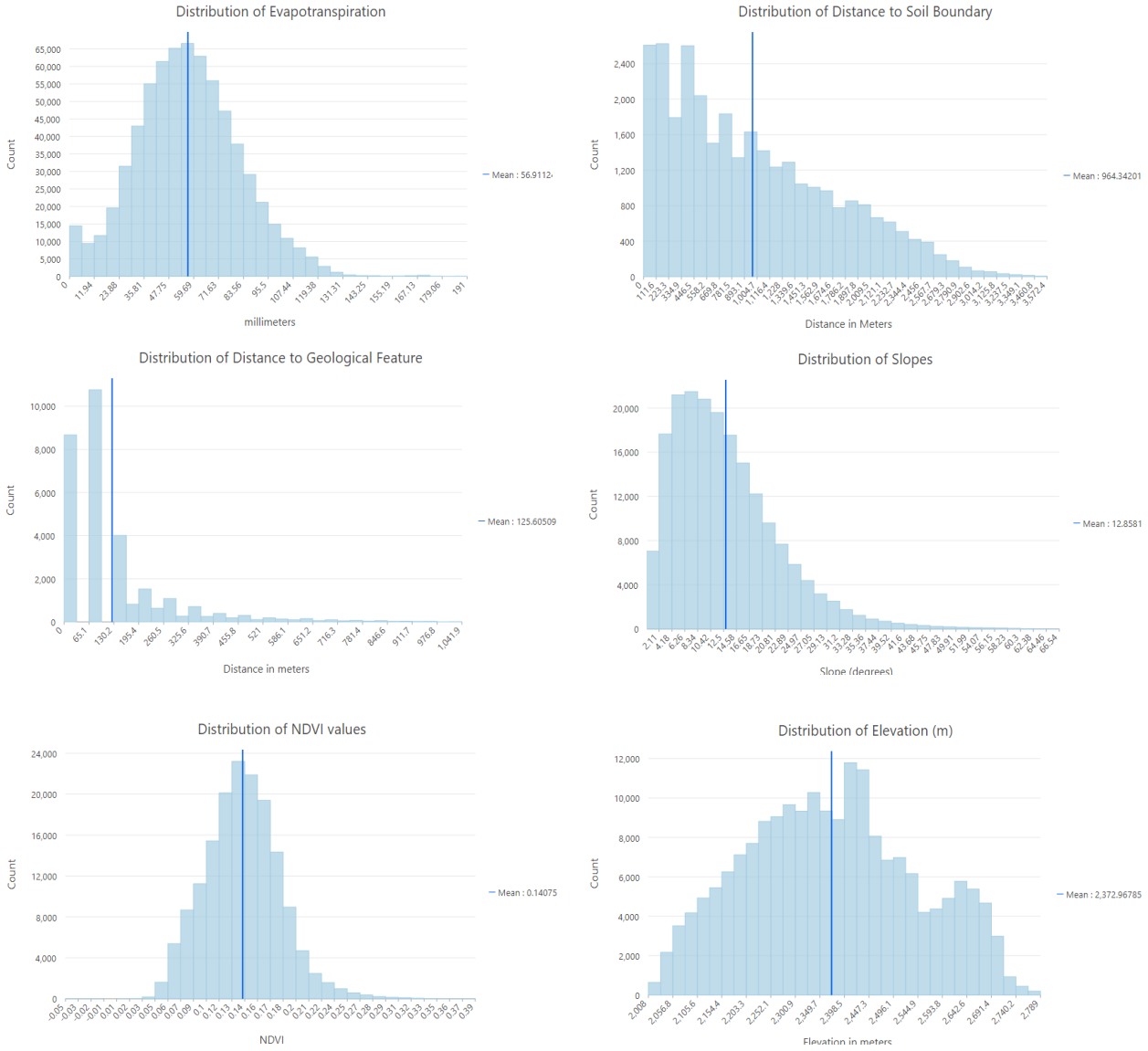

Figure A1. Distributions of Explanatory Variables

Table A2.
Summary of WLDAS Variables

Variable	Variable Abbreviation	Unit
Soil Moisture 0-10 cm, daily average	SoilMoistShallow_avg	$m^3\ m^{-3}$
Soil Moisture 10-40 cm, daily average	SoilMoist10cm_avg	$m^3\ m^{-3}$
Evapotranspiration, daily average	ET_avg	$kg\ m^{-2}\ s^{-1}$
Land Surface Temperature, daily average	SurfTemp_avg	°C
Snowfall Rate, monthly total	Snowf_sum	mm/day
Rainfall Rate, monthly total	Rainf_sum	mm/day
Snow + Rainfall Rate, monthly total	RFF_sum	mm/day
Snow Water Equivalent Rate, monthly total	SWE_sum	mm/day
Snow Sublimation, monthly total	SubSnow_sum	kg m-2 s-1

Figure A3.
Distributions of WLDAS variables

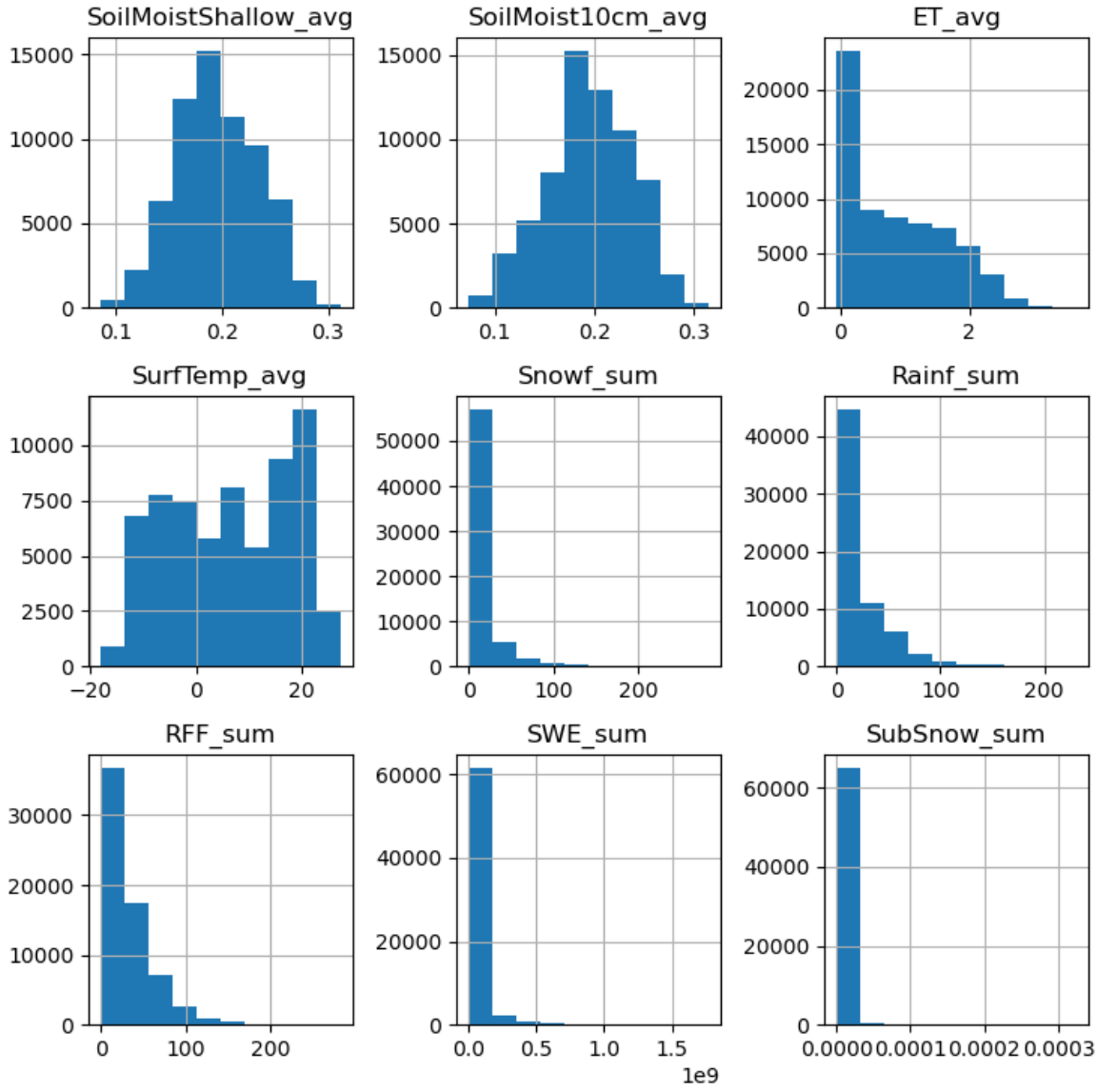

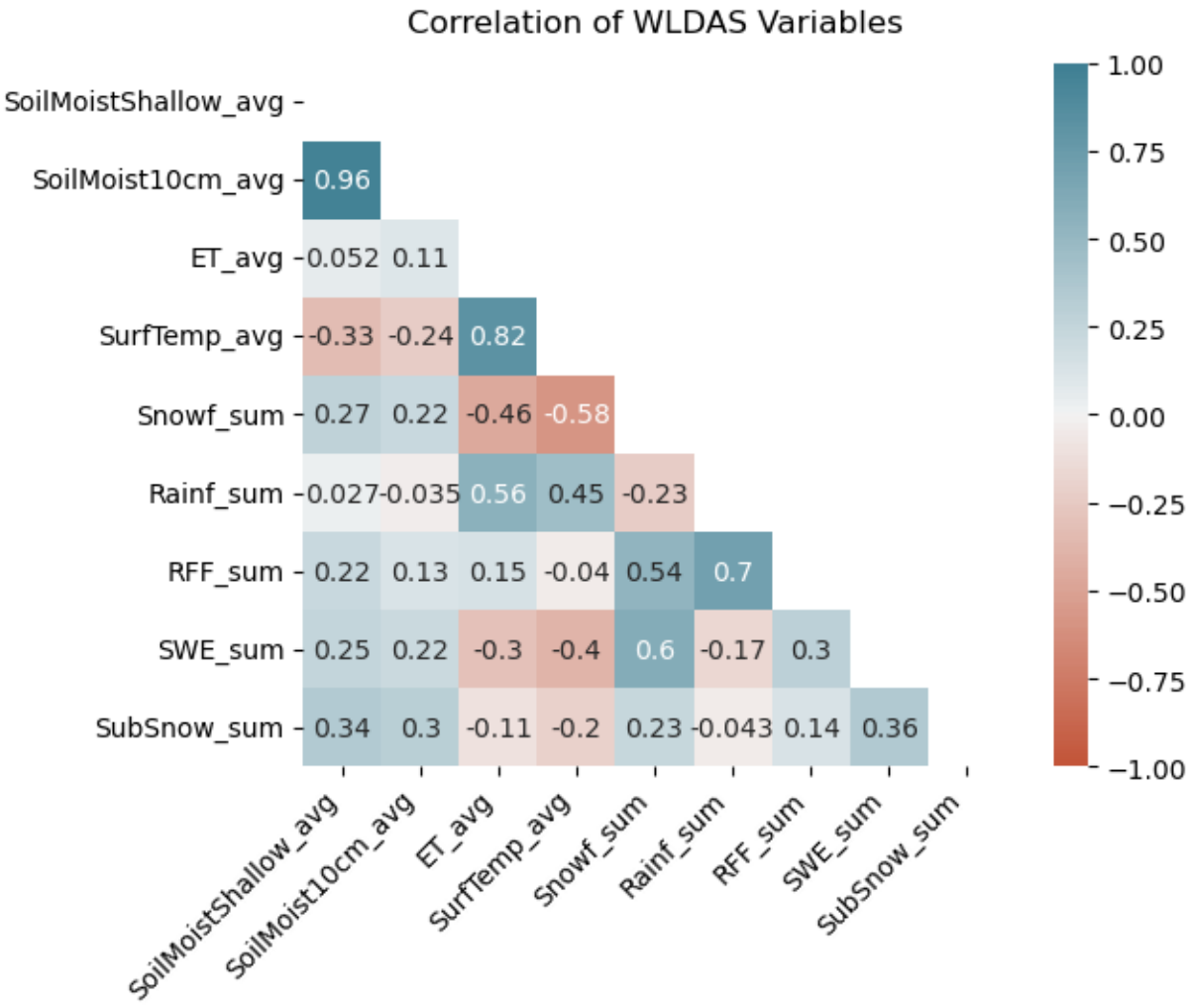

Figure A4. Correlations of WLDAS variables

Appendix B – *Results of Machine Learning Models*

Table B1.
Testing Accuracy from Random Forest Model

Accuracy of Random Forest Model		
	Seep/Spring (observed)	**Not Seep/Spring (observed)**
Seep/Spring (predicted)	56%	92%
Not Seep/Spring (predicted)	44%	8%

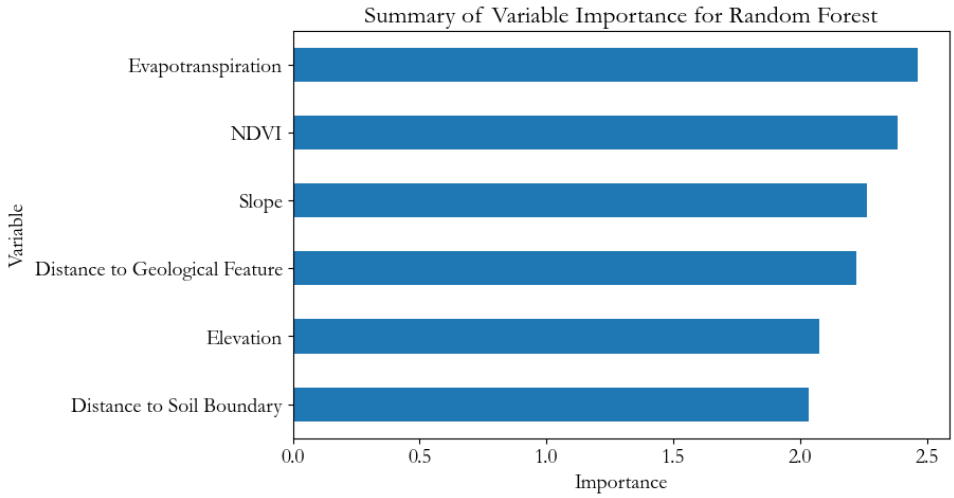

Figure B2. Variable importance for explanatory variables in the final Random Forest Model

Table B3.

Testing Accuracy from Maximum Entropy Model

Accuracy of Maximum Entropy Model		
	Seep/Spring (observed)	Not Seep/Spring (observed)
Seep/Spring (predicted)	75%	21%
Not Seep/Spring (predicted)	25%	79%

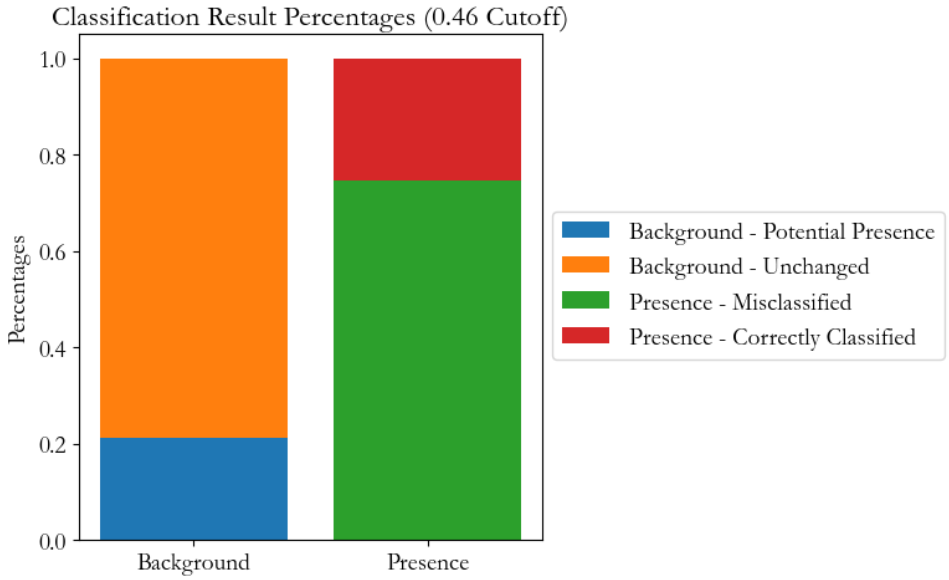

Figure B4. Classification and misclassification chart of Maximum Entropy model

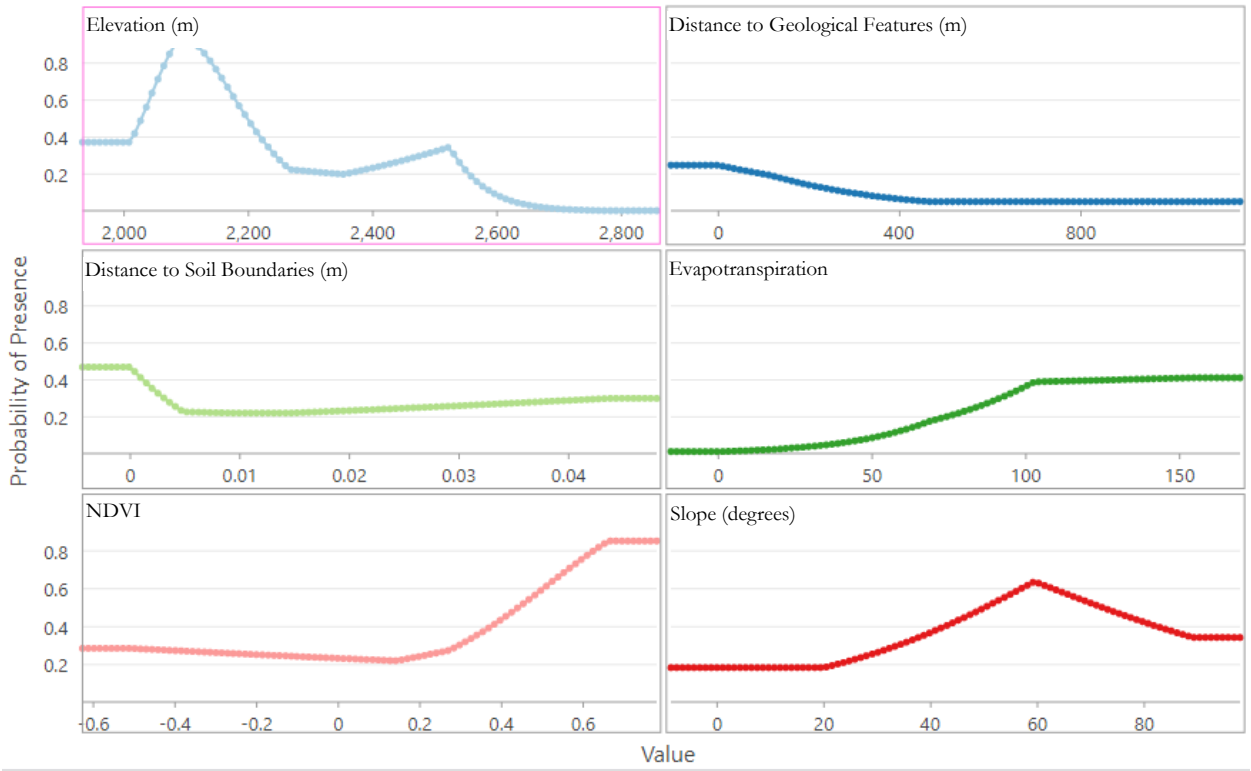

Figure B5. Maximum Entropy Model Partial Response of Continuous Variables

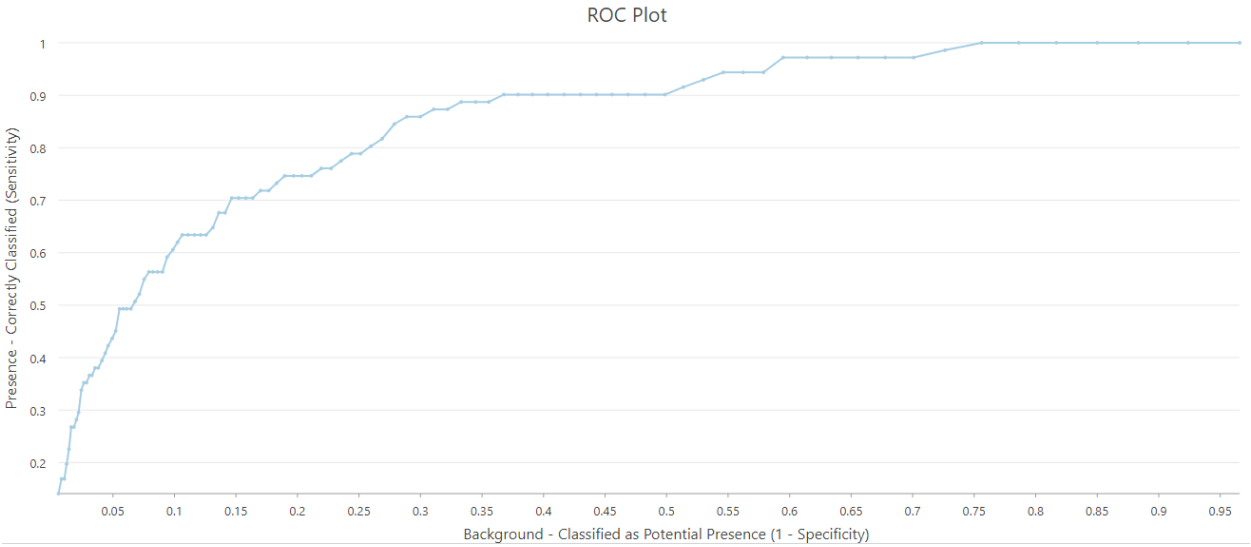

Figure B6. Response Curve of Maximum Entropy Model

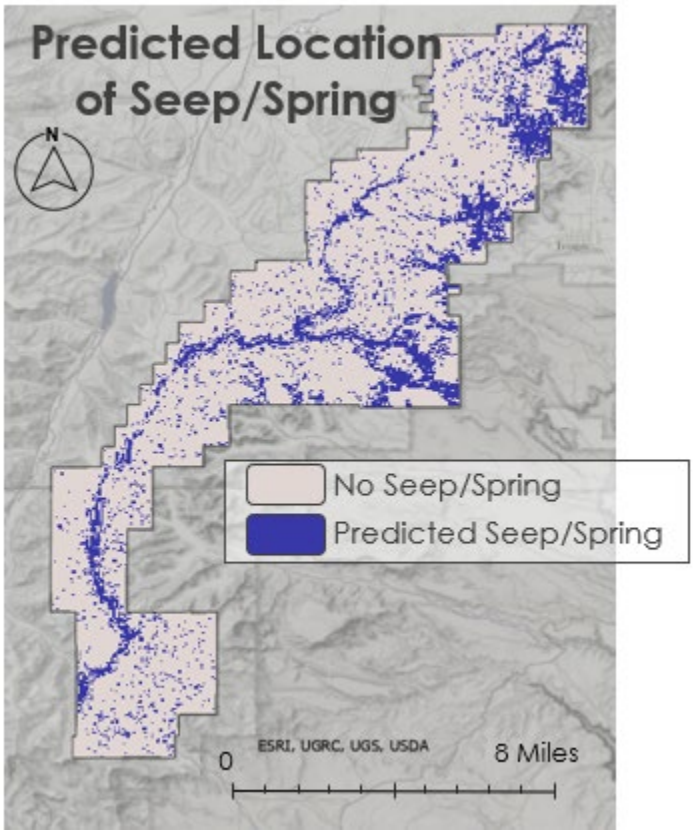

Figure B7. Random Forest Model predicted presence of seeps and springs.

Appendix C – *WLDAS climatic variable time series and in-situ time series*

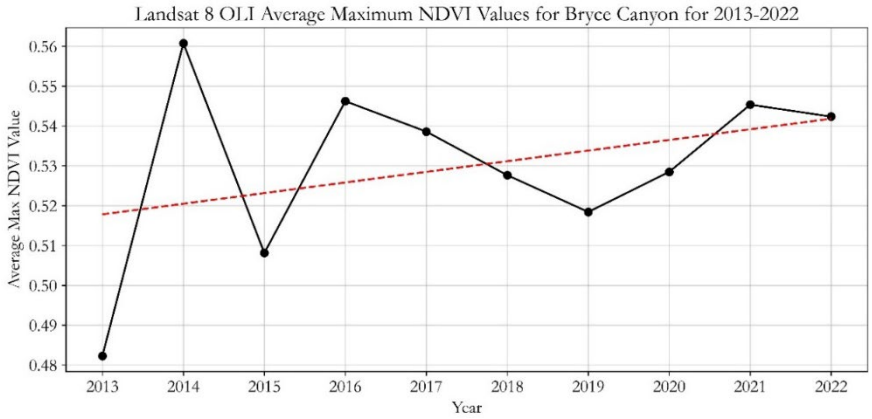

Figure C1. Time series graph of the overall trend for the average maximum NDVI values for Bryce Canyon for 2013–2022. NDVI was calculated from the red and NIR bands from Landsat 8 OLI.

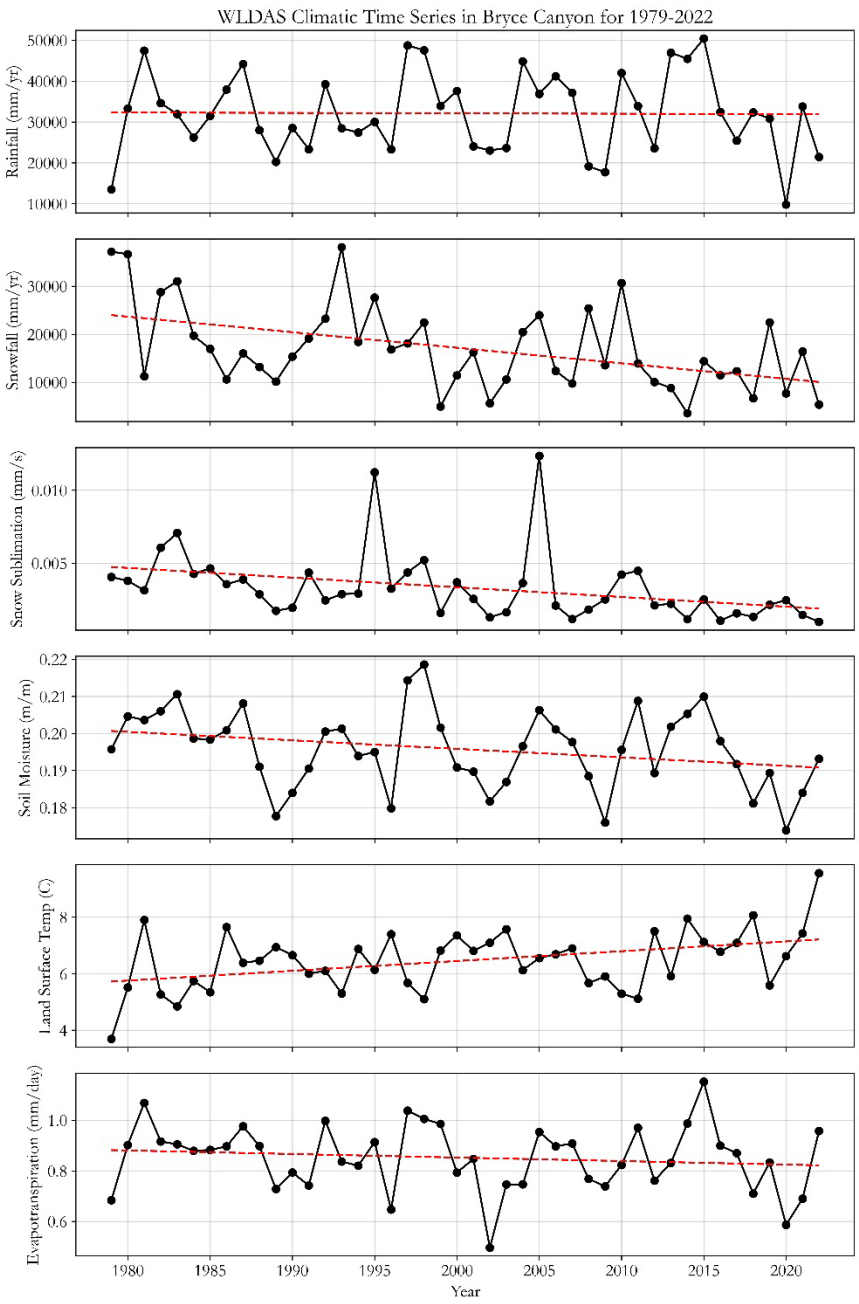

Figure C2. Time series graphs of climatic variables within Bryce Canyon. The dashed red line indicates the overall trend of the variable in the park.

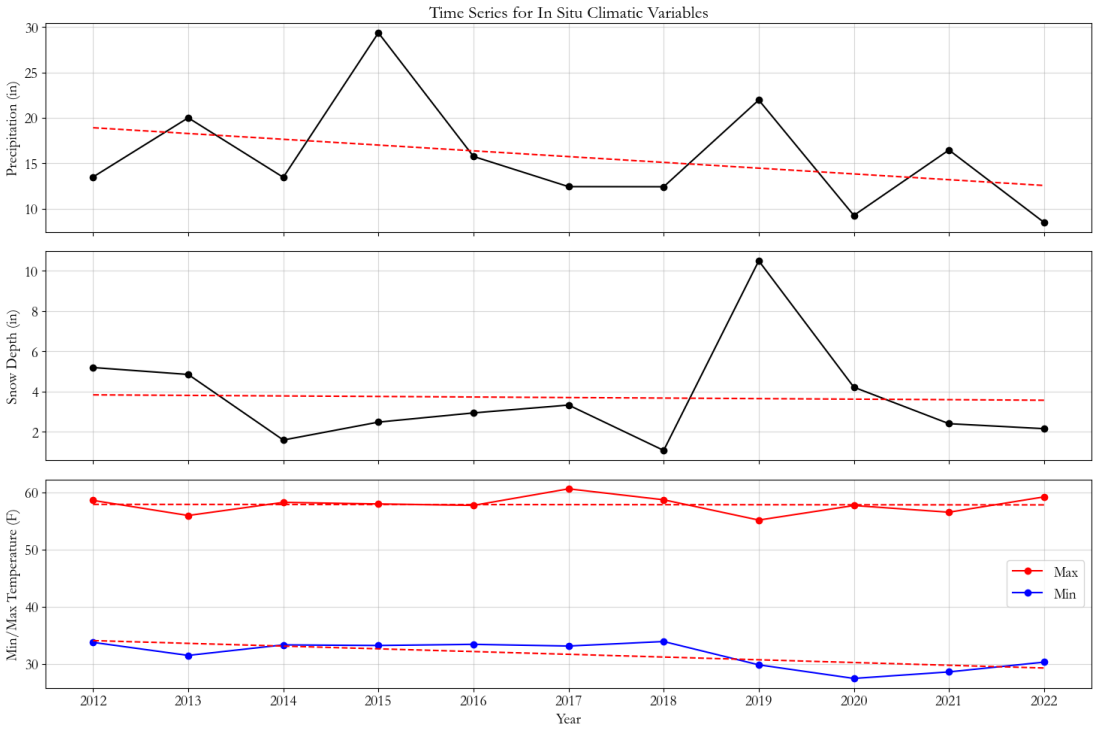

Figure C3. Time series graphs of *in situ* climatic variables within Bryce Canyon. The dashed red line indicates the overall trend of the variable in the park. Precipitation is the sum per year while min/max temperatures and snow depth is the average per year.